LANGMUIR

pubs.acs.org/Langmuir

Invited Feature Article

Seeded Growth of Plasmonic Nanostructures in Deformable Polymer Confinement

Sangmo Liu, Zuyang Ye, and Yadong Yin*

Cite This: *Langmuir* 2024, 40, 8760−8770

Read Online

ACCESS | Metrics & More | Article Recommendations

ABSTRACT: Plasmonic nanostructures exhibit optical properties highly related to their morphologies, enabling diverse applications in various areas such as biosensing, bioimaging, chemical detection, cancer therapy, and solar energy conversion. The expansive uses of these nanostructures necessitate robust and versatile synthesis methods suitable for large-scale production. Here, we introduce our recent efforts in developing a new strategy for controlling the seeded growth of plasmonic metal nanostructures, employing deformable polymer capsules to regulate the growth kinetics and the resulting particle morphology. Employing sol−gel-derived resorcinol-formaldehyde (RF) resin as a typical capsule material, we highlight its advanced features, including mechanical deformability and molecular permeability, that can be manipulated by tuning the capsule thickness and cross-linking degree. These features enable highly controllable confined seeded growth of plasmonic nanostructures. We reveal the significant role of the Ostwald ripening process of the seeds and the capsule structures in determining the morphological evolution of the plasmonic nanostructures. Moreover, we highlight some distinctive plasmonic nanostructures resulting from this unique synthesis strategy and their intriguing functionalities in various potential applications. Our discussion concludes with potential research directions to advance the development of the deformable polymer-confined seeded growth strategy into a general and robust synthesis platform for creating cutting-edge functional plasmonic nanostructures.

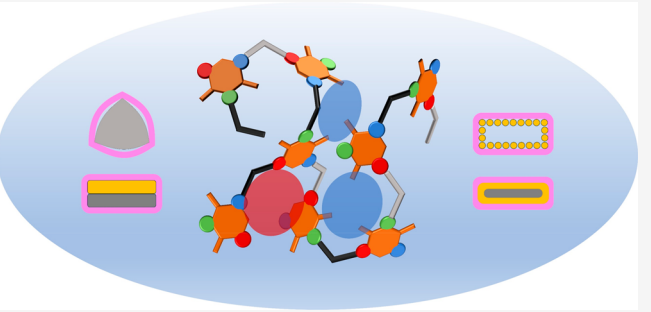

INTRODUCTION

Metallic nanostructures with localized surface plasmon resonances (LSPR) have attracted considerable research interest due to their capability to manipulate light at the nanometer scale.[1,2] They can efficiently scatter light of a particular wavelength while being "transparent" at off-resonance wavelengths,[3,4] making them important components in fabricating novel flexible transparent displays, optical metasurfaces, smart windows, wearable electronics, and color holograms.[4−10] In addition, the plasmon resonance leads to strong absorption of the incident light, converting it into heat. This photothermal effect has been widely utilized in applications ranging from tumor therapy to solar steam generation, photocatalysis, and soft actuators.[11−15] Further, the generated heat results in transient thermoelastic expansion, which produces detectable ultrasound under the illumination of high-frequency pulsed light. Therefore, plasmonic nanostructures can also serve as excellent contrast agents to enhance signals in photoacoustic (PA) bioimaging.[16,17]

An advantageous feature of plasmonic nanostructures is their shape-dependent resonance, which allows for anisotropic behaviors in both absorption and scattering due to spatially differentiated photon-electron interactions.[18,19] In brief, the light-nanostructure interaction can be described by the Mie-Gans theory, in which the absorption-affecting depolarization factor alter with the aspect ratio of the plasmonic nanostructure.[20] It enables convenient control over the plasmonic resonant frequency of the nanostructures over a broad range by simply controlling their shapes through chemical synthesis.[21−24] Further, by controlling their orientation collectively, e.g., through magnetic alignment of anisotropic nanorods hybridized with magnetic materials, one can create novel functional components that display orientation-dependent color contrast for applications in flexible displays and bioimaging,[25−29] or enable programmability in photothermal actuators that can be controlled by tunning the orientation or polarization of the light excitation.[30,31] Therefore, this shape dependence, coupled with the development of processes to enable uniform and robust synthesis and effective

Received: February 27, 2024
Revised: April 11, 2024
Accepted: April 16, 2024
Published: April 19, 2024

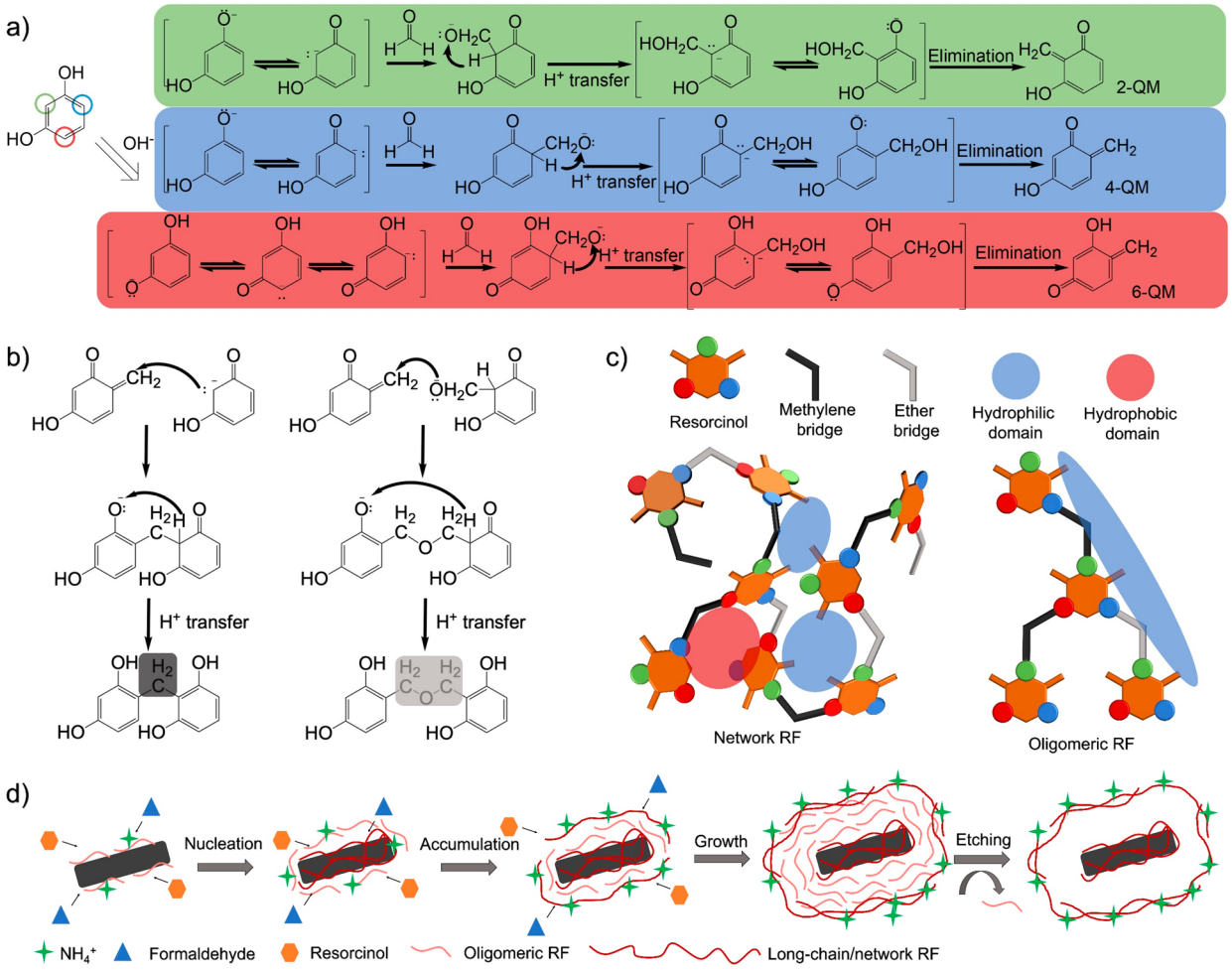

Figure 1. Chemical structure and growth mechanism of colloidal RF resin. (a) Different reaction pathways between active sites of resorcinol and formaldehyde through base-catalyzed condensation. (b) Formation of methylene bridge bonds or ether bridge bonds between QM intermediates generated from the previous step. (c) Highly cross-linked RF network and weakly cross-linked RF oligomer with high structural variety. (d) Heterogeneity of nanoscale RF shells deposited on templating substrates.

orientational alignment of the anisotropic plasmonic nanostructures, significant broadens their potential applications.

Seed-mediated growth is one of the conventional synthesis methods to prepare plasmonic metal nanostructures in controllable sizes and shapes.[32−36] Generally, metal ions (e.g., Au^{3+}, Ag^{+}) are reduced to elementary forms and deposited onto the surface of pre-existing seeds, which are usually small-sized noble metallic nanocrystals (e.g., Au, Pt) prepared in a separate process. Using seeds with different crystal symmetry and exposing crystal facets provides opportunities to tune the geometry of the final products.[37] Capping ligands are often used to selectively adsorb onto particular crystal facets of a growing nanocrystal, modifying their surface energy and manipulating their relative growth rates.[38,39] While seed-mediated synthesis has been successful in producing gold nanostructures both in laboratory and industrial settings, it exhibits limited ability to produce nanostructures with desired shapes, yield, and chemical stability from more chemically active metals such as silver and copper.[40] Additionally, the reactions are often susceptible to environmental perturbations, reducing the overall robustness of the synthesis.[41]

The challenges can be addressed by confining the growth of seeds in well-defined templates. Templating synthesis is a powerful method that uses pre-existing nanoscale spaces (e.g., silica and carbon nanotubes[23]) to guide the growth of nanostructures into desired morphologies.[42] In typical templating processes, the final morphologies of the full-grown products only depend on the internal spaces of the templates rather than the nucleation kinetics, allowing one to achieve much higher synthesis reproducibility with less operational complexity than the conventional colloidal synthesis methods, including simple seed-mediated growth processes. Meanwhile, with the availability of template materials at low cost and on a large scale (e.g., FeOOH nanorods), templating synthesis of plasmonic nanostructures can become feasible for mass production.

While previous studies primarily employed templates made of rigid inorganic materials such as silica,[23] we recently discovered some polymers, in particular resorcinol-formaldehyde (RF), that offer significant advantages over their inorganic counterparts for guiding the seeded growth of metal nanostructures.[11] These polymer-based templates feature distinct properties such as compatibility with aqueous synthesis, adjustable permeability, and shape deformability, making them especially suitable for directing metal nanoparticle growth.[31,43] The compatibility with aqueous synthesis requires the material to be hydrophilic and permeable, allowing

https://doi.org/10.1021/acs.langmuir.4c00706
Langmuir 2024, 40, 8760−8770

the diffusion of molecules and ions (e.g., metal ions and reducing agents) from the outside aqueous solution into the templates. The template also needs to be able to maintain high structural integrity during the growth process, i.e., it does not severely swell or dissolve in the solvent (typically water at various pH values). Additionally, convenient adjustment of the permeability of the template material is highly desirable for controlling the diffusion rates of the reactants, capping ligands, and byproducts to match specific growth conditions. Deformability is a unique characteristic of polymer templates that not only determines the overall shape of the grown nanostructures but also provides additional benefits. Unlike rigid templates, polymer templates can expand to accommodate the growth of seeds to a certain degree in tight spaces. Additionally, when the growing particles come into contact with the inner surface of the template, their interaction allows for selective deposition, resulting in opportunities for further manipulation of the morphology that is not possible with rigid templates.[15,44]

In this article, we aim to use RF as an example to demonstrate how to use deformable polymer templates to control the growth of plasmonic nanostructures. We will discuss the chemical structures and formation process of colloidal RF resin and then introduce the strategies to control the structural properties of RF templates, including shell thickness, cross-linking degree, and void space. By applying these strategies, we will further discuss the methods to control the structural evolution of plasmonic metal nanostructures during their growth within the confinement of deformable polymer templates. In addition to directly shaping the inner space of RF templates, these methods also include tuning reaction kinetics in seeded growth procedures by regulating growth solution compositions or RF shell structure. Finally, we showcase some unique applications enabled by the plasmonic nanostructures synthesized through this method. We conclude our discussion by providing views on future research development in this exciting synthesis strategy and the resulting plasmonic nanostructures.

DEFORMABLE POLYMER CONFINEMENT

Structure and Growth Mechanism of Colloidal RF Resins. RF resins are synthetic thermosetting polymers obtained from polycondensation of formaldehyde and resorcinol (1,3-dihydroxybenzene). With stable chemical bonds and highly cross-linked structures, bulk RF resins are durable and corrosion-resistant materials widely used as protective coatings for load-bearing structures. When reduced to the nanoscale, RF resins exhibit considerable molecular permeability and structural deformability, which are important for enabling seed growth in confined spaces.

The polymerization and cross-linking of the RF resins are typically initiated with base catalysis. As a phenol derivative, resorcinol is an acidic molecule that can be deprotonated by bases. As shown in Figure 1a, it has three active sites on the ortho positions of phenolic hydroxyl groups. Upon deprotonation of phenolic hydroxyl groups, the intermediates will be stabilized through resonance and then react with formaldehyde molecules to produce hydroxymethyl resorcinol intermediates.[45,46] This metastable form is also self-stabilized through resonance but eventually undergoes unimolecular elimination of conjugate base through the E1cB-elimination reaction under the basic environment, transforming into the quinonemethide (QM) intermediates, which are the basic building blocks for the subsequent polycondensation. It is worth pointing out that three distinct forms of QM can be produced depending on the initial deprotonation sites, as illustrated in Figure 1a, which is one of the reasons behind the structural diversity of RF resins. Another cause of structural diversity is the connections between two phenolic rings. As shown in Figure 1b, the QM intermediate can react with deprotonated resorcinol to create a methylene bridge bond (colored dark gray), or with formaldehyde-combined resorcinol to form an ether bridge bond (colored light gray), thus generating a variety of bridge bonding in the polymeric network. In addition, subsequent disproportionation can occur during condensation to transform the ether bonds into methylene bonds,[46] further enhancing the chemical stability of the RF network by preventing ether cleavage.

As shown in Figure 1c, when the three active sites on the resorcinol ring (colored according to Figure 1a) combine with the two possible bridge bonds (colored according to Figure 1b), the process of polycondensation leads to the formation of both oligomeric and cross-linked polymer networks. The complex cross-linking through strong covalent bonding provides RF resins with exceptional chemical stability. Furthermore, the tetrahedral single bonding in both methylene and ether bridge bonds offers nanoscale RF resin some freedom of molecular movement and certain overall deformability.

The structural heterogeneity of the RF also results in internal variation in the affinity to H_2O and other polar solvents. Both cross-linked and oligomeric forms of the RF resin have plenty of hydrophilic phenolic hydroxyl groups, as highlighted in light blue in Figure 1c. In contrast, the benzenoid rings and bridge bonds are hydrophobic, as labeled in light red in Figure 1c. A similar amphiphilic domain structure is also present in Novolac resins.[47−50] Although bulk RF resin is usually considered to be hydrophobic, its colloidal form allows water penetration: when the dimension is reduced to the nanometer scale, its interconnected hydrophilic domains form tunneled structures that reach the percolation threshold.[50]

The growth of RF resins through a base-catalyzed colloidal process is similar to the sol−gel process of silica, as both involve hydrolysis and polycondensation reactions to form 3D network structures.[51] Liu et al. first reported the Stöber synthesis of RF nanospheres with tunable sizes.[52] This process involves mixing polar solvents such as H_2O or H_2O/EtOH with resorcinol, formaldehyde, and ammonia, followed by emulsification. Ammonia acts as a catalyst for the polymerization reaction between resorcinol and formaldehyde, forming RF colloidal spheres. We further studied the growth mechanism in detail by depositing RF on colloidal substrates.[53] As shown in Figure 1d, the initial polymerization takes a relatively long time, depositing a thin but highly cross-linked RF layer. The growth is followed by a considerably fast polymerization reaction, depositing a relatively thick layer of RF resin primarily in oligomeric forms due to the lack of cross-linking time. As the polymerization progresses and most monomers are consumed, the growth process slows considerably, leading to a more cross-linked outer layer. This hierarchical structure was confirmed by selectively etching the oligomeric regions using EtOH or other polar solvents. The resulting yolk−shell structures provide evidence of a varying degree of cross-linking throughout the thickness of the shell, as illustrated in Figure 1d.[53]

https://doi.org/10.1021/acs.langmuir.4c00706
Langmuir 2024, 40, 8760−8770

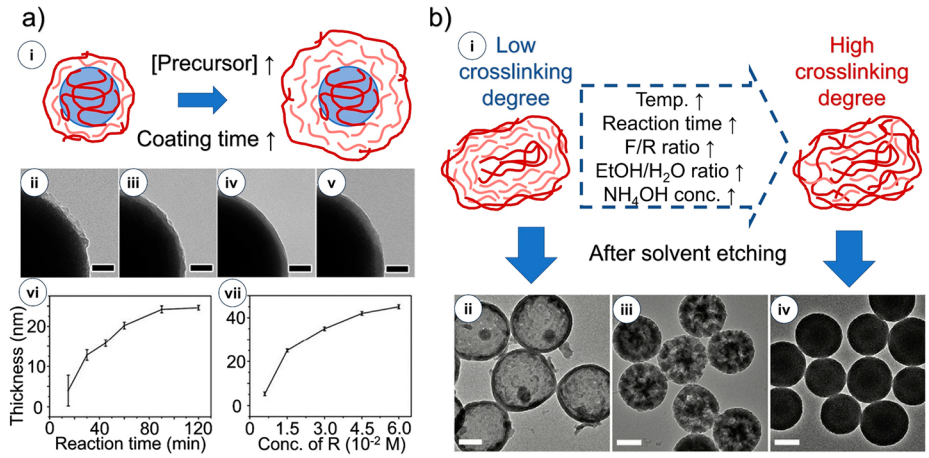

Figure 2. Structure tuning of RF capsules. (a) Methods for attaining effective RF coating on template nanostructures and regulating coating thickness: (i) schematic illustration of RF coating, (ii-v) TEM images of SiO_2 nanoparticles with increasing RF shell thicknesses, (vi, vii) Dependence of RF thickness on reaction time (vi) and precursor concentration (vii). Scale bars are 50 nm. Reprinted with permission from ref 54. Copyright 2013 Royal Society of Chemistry. (b) Regulation of cross-linking degrees of RF capsules: (i) dependence of cross-linking degree on various experimental parameters (F and R indicate formaldehyde and resorcinol, respectively), (ii-iv) TEM images of RF spheres condensed in different degrees and then etched by EtOH. Scale bars are 200 nm. Reprinted with permission from ref 53. Copyright 2020 Royal Society of Chemistry.

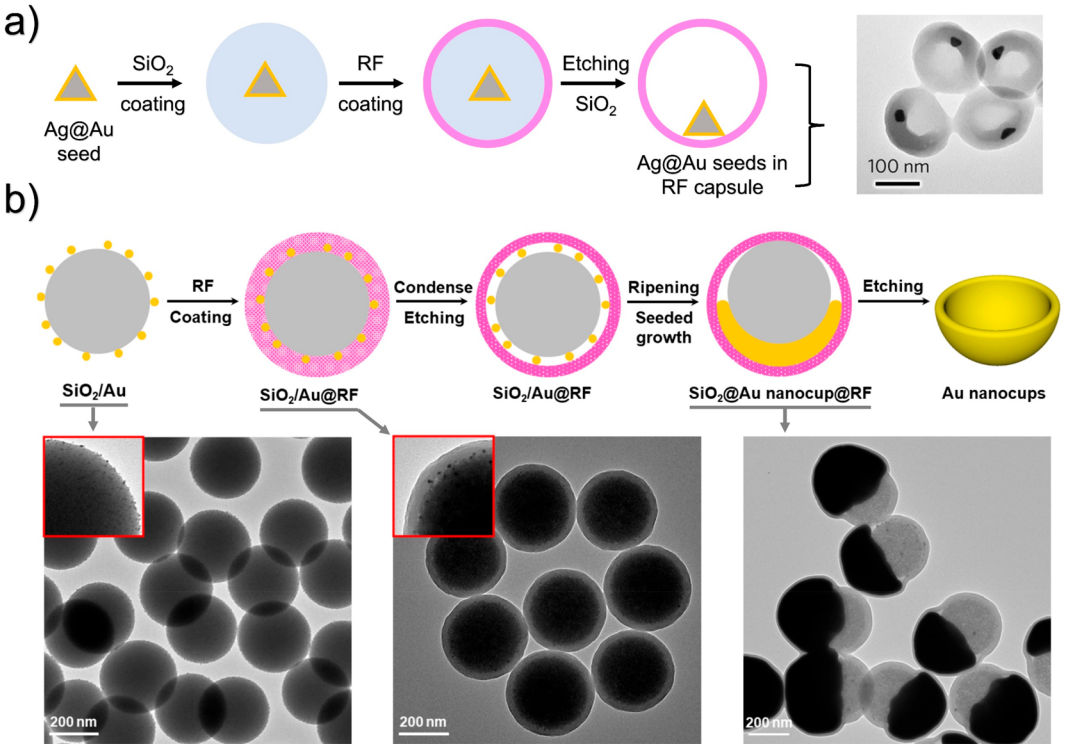

Figure 3. Generating spaces for confined seeded growth. (a) Creation of growth space by depositing SiO_2 (sacrificial material) on seeds (e.g., Ag@Au nanoplates) followed by coating an RF shell and then selective etching of SiO_2. The thickness of the SiO_2 layer can be varied to control the spaces available for seeded growth of the plasmonic nanostructures within RF capsules. Reprinted with permission from ref 44. Copyright 2020 Wiley-VCH GmbH. (b) Creation of space with dual-confinement capability by partially etching the SiO_2 layer before subsequent seeded growth of Au nanocups. Reprinted with permission from ref 56. Copyright 2022 The Author(s). Published by Elsevier Ltd.

Shaping Polymer Capsules for Confined Growth. The polymer confinement is formed by coating a layer of RF resin onto the templating substrates. The formed RF resins are negatively charged after being deprotonated during the synthesis using the Stöber method. However, coating RF on templates with negatively charged surfaces such as SiO_2 nanoparticles may become challenging due to electrostatic repulsion, resulting in the formation of free RF spheres. To overcome this problem, one can modify the template surface with cationic ligands such as cetyltrimethylammonium bromide (CTAB) to enhance its affinity to RF through electrostatic attraction and enable successful conformal coating.[54] For the following space-confined seeded growth, the thickness of the RF capsule is an important parameter that

https://doi.org/10.1021/acs.langmuir.4c00706
Langmuir 2024, 40, 8760−8770

affects the permeability and deformability of shells.[43] For example, thicker RF shells are more difficult to deform and generate percolated hydrophilic domains. The shell thickness can be tuned by adjusting the reaction time or the concentration of RF precursors (with a fixed ratio of resorcinol to formaldehyde), as illustrated in Figure 2a(i). The transmission electron microscopy (TEM) images (Figure 2a(ii-v)) indicated that RF shell thickness on 360 nm SiO_2 spheres could be increased by elongating reaction time from 15 to 90 min. Figure 2a(vi) provides quantitative results of RF shell thickness tuning controlled by reaction time. Additionally, by simply altering the concentration of resorcinol from 0.6 mM to 6.0 mM, the thickness of the RF shell could also be varied from ∼5 nm to ∼45 nm (Figure 2a(vii)).

The permeability and deformability of capsules depend on not only the thickness but also the cross-linking degree of the polymer. As discussed above and illustrated in Figure 2b(i), an RF shell is effectively a network of polymer domains with varying cross-linking degrees resulting from the different concentrations of resorcinol and formaldehyde during polycondensation.[55] Local insufficiency of formaldehyde may produce oligomeric domains within otherwise highly cross-linked networks. Deprotonation with bases (e.g., NaOH) or solvation with polar solvents (e.g., dimethylformamide (DMF)) may remove the oligomers, leaving behind a highly cross-linked RF polymer framework. For RF shells with weak cross-linking, an extensive etching with solvent will eventually cause the loss of structural integrity (Figure 1d and Figure 2b(ii)). The dissolved oligomeric RF was further verified through Matrix-Assisted Laser Desorption/Ionization Time-of-Flight (MALDI-TOF) mass spectrometry (MS).[53] In contrast, RF shells with increasing degrees of initial cross-linking can maintain higher structural integrity after etching, as shown in the TEM images in Figures 2b(iii) and (iv). However, losing oligomers reduces their mechanical strength and makes them more flexible, allowing less strict confinement to the growth of the plasmonic nanostructures.[43] On the other hand, the etching process creates more hydrophilic domains within the shells, further enhancing the permeation of precursors and other species involved in the seeded growth. Therefore, the growth kinetics and the final morphology of the plasmonic nanostructures can be conveniently controlled by tuning the initial cross-linking degree of the RF shells or the extent of subsequent etching.

Similar to the cases with rigid confinement, the morphologies of grown plasmonic nanostructure are determined largely by the available spaces defined by the RF capsules.[42] As RF resin wraps the templating substrates and faithfully replicates their shape, the spaces available for seeded growth can be controlled by starting with sacrificial templates of different sizes[44] and aspect ratios.[15] As an example shown in Figure 3a, citrate ion-capped Ag@Au nanoplates could be coated with silica of desired thicknesses. After being further coated with an RF shell, the silica sacrificial layer could be etched with HF or NaOH, generating controllable spaces for growing seed particles. In addition to silica, a large variation of sacrificial templates (e.g., nickel-hydrazine complexes, FeOOH, and Fe_3O_4) can be used due to the relatively strong resistance to acids and bases of highly cross-linked RF capsules.

We want to highlight that the sacrificial templates do not have to be removed entirely before seeded growth. In fact, they can be either kept intact or partially etched and then combined with the deformable RF capsules to provide dual confinement (Figure 3b). For example, coating RF onto Au seed-decorated SiO_2 spheres requires a basic environment, which causes slight etching of SiO_2 and generates a small gap between the SiO_2 template and the RF shell. Upon enhanced Ostwald ripening, the Au seeds are drastically reduced to minimum numbers. The growth of such seeds under the dual confinement of the SiO_2 sphere and RF shell occurs predominantly on one side of the space, producing cup-shaped Au nanostructures that can be released after removing the SiO_2 and RF templates.[56] In another example, Fe_3O_4 nanorods (NRs) are enclosed in RF capsules to provide dual confinement to create tunable surface concavity in Au nanorods, enabling unique opportunities for controlling their plasmonic properties.[27,43]

Compared to rigid counterparts, polymer capsules are often deformable, a unique property that enables regulating the adaptive growth of anisotropic nanostructures.[15,44] We have demonstrated this feature by using spherical RF capsules to control the anisotropic growth of triangular Ag nanoplates (Figure 4a).[44] The Ag nanoplate seeds contain a stacking fault

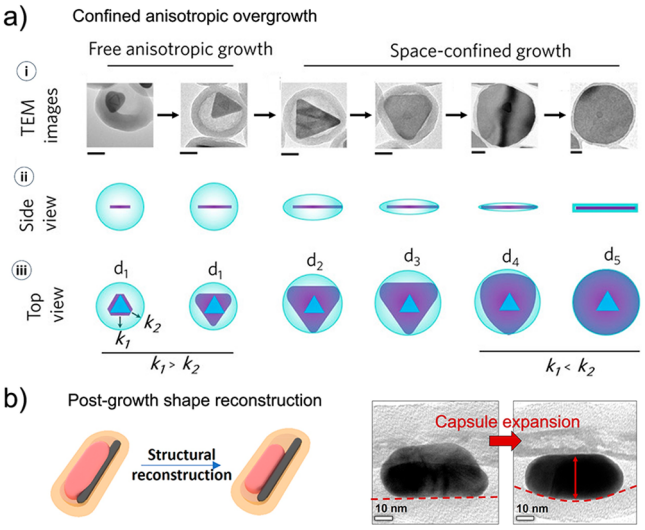

Figure 4. Adaptive seeded growth mediated by deformable RF confinement. (a) Anisotropic growth process of Ag nanoplate seeds in RF capsules: (i) TEM images showing the growth of an Ag nanoplate at different stages in an RF nanoshell. The scale bars are all 50 nm. (ii, iii) Illustration of the shape evolution of the Ag nanoplate and RF shell in side and top views. k_1 and k_2 represent the rate constants of the growth on the sides and edges of the Ag@Au nanoplate seed, respectively. Reprinted with permission from ref 44. Copyright 2020 Wiley-VCH GmbH. (b) Postgrowth reconstruction of plasmonic nanostructure (pink rod) through thermal ripening and expansion of deformable RF capsule in the presence of adjacent Fe_3O_4 NR (black rod). Reprinted with permission from ref 43. Copyright 2021 American Chemical Society.

that promotes their lateral growth. They grow continuously into triangular nanoplates in the early growth stage. As the vertices of the triangles approach the inner surface of the RF shells, the shells deform to enable the continued anisotropic expansion of the nanoplates. When the shells are fully stretched, the predominant growth switches to the sides of the triangles, eventually resulting in circular Ag nanoplates tightly bound by the deformed RF shells. At this stage, the RF acts as polymeric capping ligands, providing additional protection to the Ag nanoplates against oxidative etching

https://doi.org/10.1021/acs.langmuir.4c00706
Langmuir 2024, 40, 8760−8770

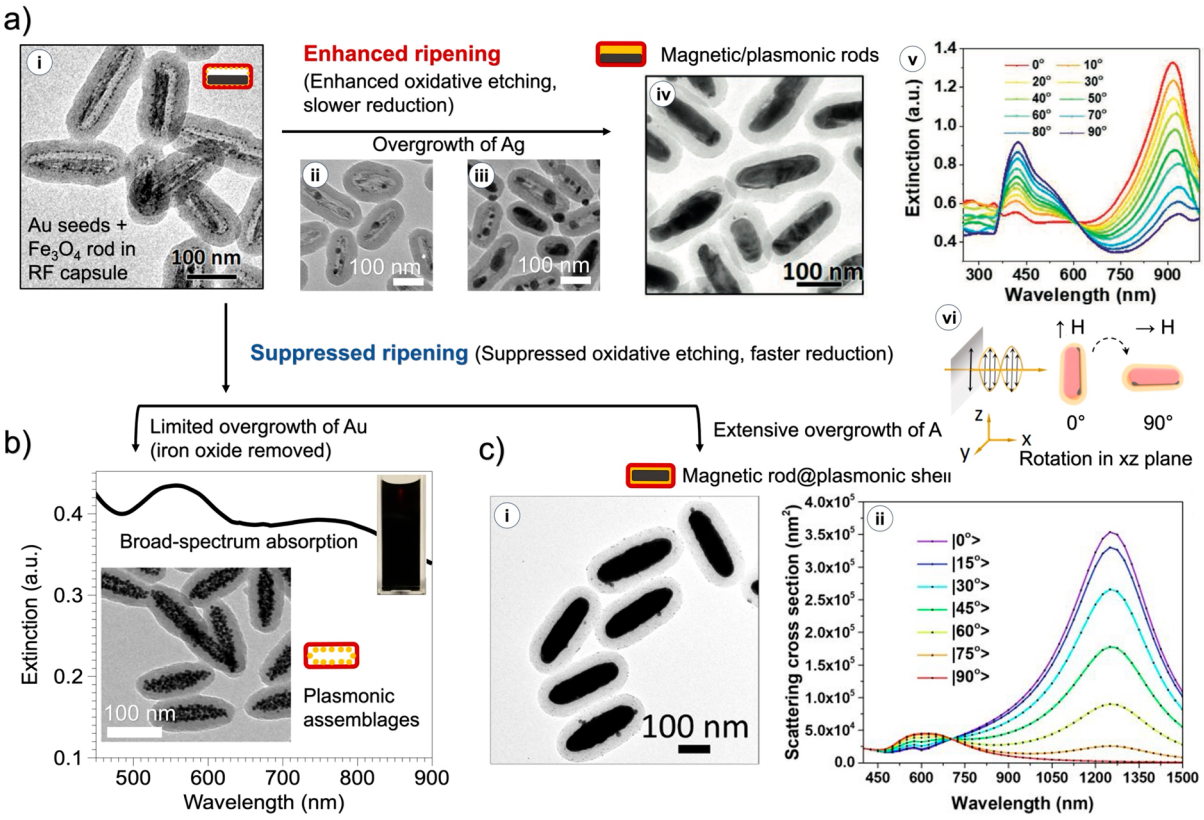

Figure 5. Morphological control of plasmonic nanostructures by tuning Ostwald ripening. (a) Enhanced ripening of seeds for growing Fe_3O_4/Ag magnetic/plasmonic hybrid nanorods. Image (i) shows the initial Au seeds/Fe_3O_4 nanorods encapsulated in RF capsules. The number of Au seeds is greatly reduced through enhanced Ostwald ripening, which is achieved by promoting their oxidative etching. Images (ii-iv) show the gradual formation of an Ag nanorod beside a Fe_3O_4 nanorod in each RF capsule upon the overgrowth of Ag on the ripened seeds. Panel (v) shows the magnetic tuning of the plasmonic excitation of the hybrid nanorods by controlling their orientation relative to the incident polarized light; Panel (vi) illustrates the definition of NR's relative angle to polarized light. Reprinted with permission from ref 31. Copyright 2020 Wiley-VCH GmbH. (b) Suppressed ripening of seeds for growing Au nanoassemblages. The number of Au seeds is maintained by suppressing their Ostwald ripening. Limited overgrowth of Au on the seeds produces plasmonic nanoassemblages (image shown in the left inset) with broad-spectrum absorption, as evidenced by the black color of their dispersion in the right inset. Reprinted with permission from ref 11. Copyright 2018 American Chemical Society. (c) Suppressed ripening of seeds for growing Fe_3O_4@Au core−shell magnetic/plasmonic nanorods. Extensive overgrowth of Au on the seeds produces core−shell structures (i) that display magnetically tunable scattering properties under the irradiation of polarized light (ii). Reprinted with permission from ref 28. Copyright 2022 American Chemical Society.

through the reductive property of the resin and its ability to limit oxygen diffusion to the silver surface.

The deformability of the polymer templates offers many possibilities for controlling the morphologies of metal nanostructures and their plasmonic properties. Even after the growth, the RF shells can still be deformed to accommodate the shape reconstruction of the grown plasmonic nanostructures. Figure 4b demonstrates such a case where a concave Au nanorod, confined in an RF shell, changes shape as a result of heat-induced ripening.[43] To allow more substantial shape reconstruction of the encapsulated metal nanostructures, one may simply enhance the deformability of the RF shells by partially etching them with polar solvents.

Regulating Reaction Kinetics of Seeded Growth Processes. The morphology of attained plasmonic nanostructures can be tuned by controlling the kinetics of the seed ripening process, in addition to the shape of RF capsules. Specifically, one can regulate the reaction rates of oxidative etching of metal atoms and the reductive deposition of metal ions, two key steps involved in the Ostwald ripening of the seeds.

Encapsulating a precisely controlled number of seeds within a polymer shell remains challenging. In cases where the growth is preferred from a single or small number of seeds, promoting Ostwald ripening of the seeds is essential, such as with nanorods and nanocups. In our previous attempt to grow an Ag nanorod alongside a magnetite nanorod confined within an RF shell, we raised the growth temperature to 80 °C to enhance the oxidative etching of Au seeds during the early stage of the reaction, leading to decreased numbers but enlarged sizes of the seeds.[31] The oxidative etching was further facilitated by adding complexing agents, such as KI, to the system.[27,43,56] According to Le Chatelier's principle, the oxidation of gold would be promoted by the complexation of reaction products (gold cations) with the ligands.[57] The ripening significantly reduced the number of seeds and allowed them to grow upon introducing the silver precursor into a complete nanorod. Such a seeded growth scheme ensures the formation of an Ag nanorod next to the magnetite nanorod, as indicated in Figure 5a(i-iv), rather than an Ag shell encapsulating the magnetite nanorod. The high shape-anisotropy of the Ag nanorods enables different absorption and scattering cross sections along longitudinal and transverse

https://doi.org/10.1021/acs.langmuir.4c00706
Langmuir 2024, 40, 8760−8770

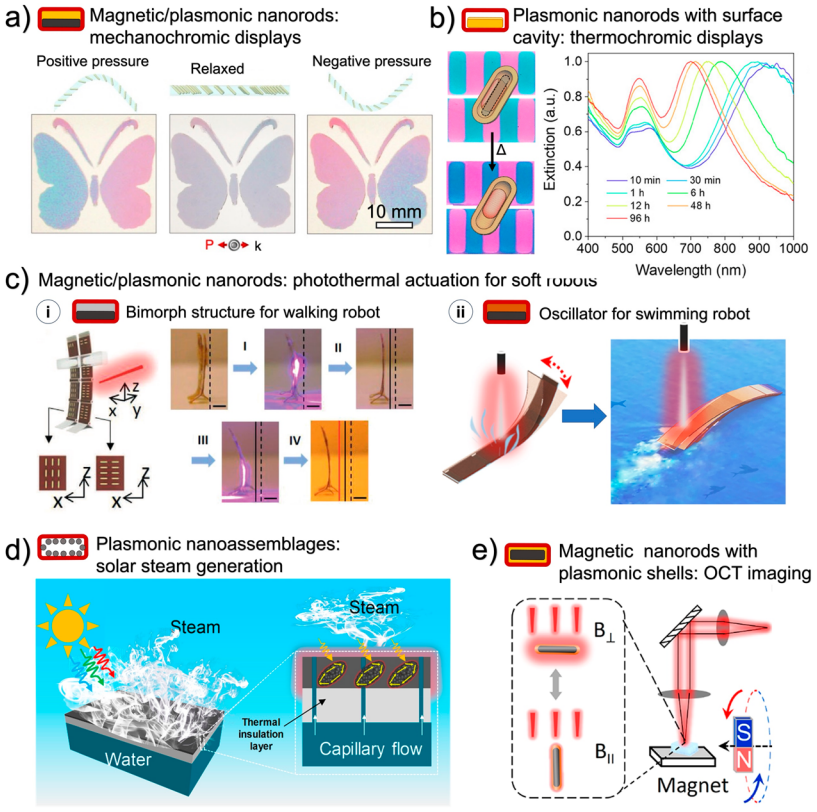

Figure 6. Applications of plasmonic nanostructures prepared by RF-confined seeded growth. (a) Pressure-sensitive mechanochromic display fabricated using magnetically aligned magnetic/plasmonic hybrid nanorods. **P** and **k** are the polarization and wave vectors of the incident light, respectively. Reprinted with permission from ref 27. Copyright 2020 The Author(s). (b) Thermochromic display fabricated using plasmonic nanorods with energetic surface concavity. Thermal-treatment-time-dependent extinction spectra are included. Reprinted with permission from ref 43. Copyright 2021 American Chemical Society. (c) Untethered photothermally driven soft robots with various motion modes fabricated using magnetic/plasmonic hybrid nanorods: (i) walking robot based on photothermal actuation of bimorph structures, (ii) swimming robot based on oscillation driven by photothermal steam generation. Scale bar is 5 mm. Reprinted with permission from ref 31. Copyright 2020 Wiley-VCH GmbH. Reprinted with permission from ref 60. Copyright 2021 The Authors, some rights reserved; exclusive licensee American Association for the Advancement of Science. No claim to original U.S. Government Works. (d) Photothermal solar energy harvesting and water steam generation achieved by plasmonic nanoassemblages with broad-spectrum absorption. Reprinted with permission from ref 11. Copyright 2018 American Chemical Society. (e) Background-free OCT imaging enabled by magnetically modulating the plasmonic excitation of magnetic/plasmonic core–shell hybrid nanostructures. Reprinted with permission from ref 28. Copyright 2022 American Chemical Society.

directions.[15] As discussed more in the Application section, the magnetic/plasmonic hybrid nanorods feature polarization/wavelength-dependent plasmon excitation that can be tuned by magnetically controlling the nanorod orientation relative to the incident angle and polarization direction of the light (Figure 5a(v)).[27,31,43]

In cases where maximum plasmonic coupling is desired, Ostwald ripening must be suppressed in order to maintain the number of seeds during their growth. Typically, the seeded growth is implemented at a mild temperature without complexing agents like KI.[11,58] The oxidative etching of Au seeds can therefore be suppressed. Without significant ripening, the reduced metal atoms will be uniformly deposited onto the seed surface, increasing their sizes, decreasing interparticle distances, and strengthening their plasmonic coupling. This growth process will then lead to plasmonic assemblages with large absorption cross sections that can maximize the absorption of incident visible and near-IR light (Figure 5b). More importantly, since the seeds are loaded inside the tubular space without any specific order, the interparticle coupling could happen along either longitudinal or transverse directions, leading to random plasmonic coupling and consequent broad-band absorption.[11,58] On the other hand, extensive seed growth eventually merges all nanoparticles into complete shells (Figure 5c(i)), producing core–shell nanorods that exhibit different absorption and scattering profiles than assemblages.[5,59] If the Fe_3O_4 nanorods are kept within the RF capsules during the seeded growth, the resulting hybrid nanorods also feature magnetically tunable plasmonic resonance, as shown in Figure 5c(ii).

APPLICATIONS

The seeded growth process confined within deformable polymer capsules offers new opportunities to create plasmonic nanostructures with unique morphologies and properties, opening the door to various novel applications. In particular, we have explored the use of magneto/plasmonic hybrid nanorods for stimuli-responsive displays by taking advantage of their orientation-dependent plasmonic properties that can be controlled using external magnetic fields. Figure 6a shows a film of butterfly pattern created by embedding these hybrid nanorods within a hydrogel film, with the nanorod magnetically aligned 45° to the surface normal.[27] When subjected to pressure, the film bends upward or downward, exhibiting

https://doi.org/10.1021/acs.langmuir.4c00706
Langmuir 2024, 40, 8760−8770

asymmetric mechanochromic responses in the two wings of the butterfly due to the excitation of different plasmon modes of the nanorods.

Figure 6b illustrates the case where dual confinement of Fe_3O_4 NRs and RF capsules can be manipulated to create a unique surface concavity in the Au nanorods,[27,31,43] Such a surface concavity produces an additional transverse resonance mode that is dominated by scattering.[43] The high surface energy associated with the concavity allows the nanorods to reconstruct even at a moderate temperature (Figure 4b), inducing a blueshift of the concavity band and exhibiting thermal responsive color changes. We have explored this temperature-dependent structural reconstruction property to fabricate thermochromic plasmonic films that can display patterns with vivid color changes and reveal encrypted information upon aging (Figure 6b).

Anisotropic excitation of plasmonic nanorods can also lead to polarization/wavelength-dependent photothermal conversion, which is useful in designing untethered actuators. In our previous work, a general design involves a three-layer bimorph structure, with a middle polyacrylamide (PAM) layer containing magnetically aligned plasmonic-magnetic hybrid nanorods sandwiched between polydimethylsiloxane (PDMS) and polyimide (PI) layers.[15] The hybrid nanorods in the middle layer convert light into heat, causing the PDMS and PI layers to expand at different rates due to their different thermal expansion coefficients (CTEs). Taking advantage of the different absorption/excitation modes of longitudinal and transverse modes of plasmonic nanorods (Figure 5a), we have designed a bimorph photothermal actuator with two legs made of films containing Fe_3O_4/Ag NRs aligned in orthogonal directions, as illustrated in Figure 6c. The legs can be selectively heated by a 450 nm pulsed laser with controlled polarization to induce forward bending.[31] Alternating the polarization direction of the laser makes it possible to achieve not only simple stepping but also turning.

The confined seeded growth process can be extended reliably for synthesizing anisotropic Cu nanostructures, which are otherwise difficult to make with conventional methods due to the complications associated with the relatively low reduction potential (thus the ease of oxidation) of Cu.[41] In addition to directing the shape of the Cu nanostructures, RF confinement also enhances their chemical stability against oxidation, thanks to the reductive nature of the polymer. With the added benefit of low cost, the as-synthesized Cu nanorods can serve as excellent photothermal agents with performance comparable to their Au and Ag counterparts. We recently incorporated Cu nanorods into triple-layer actuators to enable soft robots to climb stairs or swim on water surfaces.[15,60] In particular, the swimming robot was built based on the mechanical perturbation associated with the formation and collapse of steam bubbles driven by the photothermal heating of the water by Cu nanorods embedded in the middle hydrogel layer, as illustrated in Figure 6c.

The assemblages of plasmonic nanoparticles grown with suppressed ripening feature distinct optical properties, making them useful for many niche applications. The significant plasmonic coupling results in broad-spectrum absorption, leading to extremely high efficiency of photothermal conversion (e.g., 95.2% for Ag assemblages,[11] 83.7% for Au assemblages[58]). Such exceptional photothermal conversion capabilities build robust foundations for their applications. For instance, confined-grown plasmonic nanoassemblages can be candidate materials for efficient solar steam generation, as illustrated in Figure 6d.[11] Leveraging the photothermal effect to produce clean water, such technologies are becoming increasingly popular methods to combat global water scarcity and have shown significant promise in enhancing water availability. In addition, their extremely high photothermal conversion efficiency can be applied in photothermal therapy for cancer treatment, further demonstrating their technological importance.[58]

Extensive seeded growth eventually leads to the formation of plasmonic nanoshells, with their optical properties dominated by scattering. Incorporating a magnetic core within each nanoshell produces magnetic/plasmonic hybrid nanoshells that can be assembled into linear chains under an external magnetic field. Featuring magnetically tunable plasmonic coupling and resonant scattering, such nanoshell chains have been employed in designing unique transparent displays and anticounterfeiting devices.[61] For ellipsoidal magnetic/plasmonic core−shell nanostructures, the excitation of resonant scattering and absorption depends on their orientations, which can be magnetically controlled (Figure 5b).[28,29] Recently, we demonstrated the use of Fe_3O_4@Au NRs as active contrast agents for optical coherence tomographic (OCT) imaging, generating strong scattering signals by magnetically switching on their longitudinal resonance mode (Figure 6e).[28] In another effort, we have shown that the strong absorption associated with their longitudinal mode can lead to local heating, producing ultrasound signals for photoacoustic imaging when a pulsed laser is used as the light source.[29] In both cases, the imaging modalities can be enhanced or deactivated by controlling the nanorod orientation using magnetic fields, allowing effective minimization of background noises through simple pixel subtraction. Furthermore, the rapid and dynamic magnetic response of Fe_3O_4@Au NRs makes it possible to generate periodic signals under an alternating magnetic field, enabling automatic screening of NRs signals from the random biological noises and reconstruction of fast Fourier transform (FFT)-weighted, background-free images using a computational algorithm based on a time-sequence image set.[28,29]

CONCLUSIONS AND PERSPECTIVES

By confining the seeded growth process within deformable polymer nanoshells, we can enhance the reproducibility of synthesis processes for plasmonic nanostructures in comparison to direct colloidal synthesis. Furthermore, this approach offers additional control and flexibility over their morphologies when contrasted with hard templating methods. Additionally, it facilitates the creation of hybrid nanostructures, particularly those that integrate magnetic and plasmonic components, which has remained a challenge for direct colloidal synthesis methods. Therefore, this synthesis technique not only boosts the robustness of plasmonic nanostructure synthesis but also introduces morphological diversity and enables multifunctionality in the resulting products.

Polymers used for confining the seeded growth must have specific characteristics such as chemical stability, cross-linked network structure, deformability, amphiphilicity, and permeability that can be conveniently controlled. These properties are necessary for the polymer confinement to maintain its structural integrity while allowing the growth precursors to penetrate and regulating the morphology of growing nanostructures through adaptive deformation. We have identified RF resin, a member of the phenolic resin family, as

https://doi.org/10.1021/acs.langmuir.4c00706
Langmuir 2024, 40, 8760−8770

a good option due to its permeability and deformability that can be controlled by adjusting its thickness and cross-linking degree. By regulating the growth solution compositions and the polymer confinement, we can finely control the growth kinetics of nanostructures to generate plasmonic building blocks that meet specific application requirements. We can also increase the variety of plasmonic nanostructure morphologies by adding templates inside the polymer shells to regulate their shapes. This synthesis method has proven effective in creating plasmonic nanostructures with variable compositions (Au, Ag, and Cu) and morphologies (assemblages, shells, rods, and cups) with unique plasmonic properties and added multifunctionalities. The resulting plasmonic nanostructures have found intriguing applications such as stimuli-responsive chromic displays, photothermal therapy, photothermal actuation, and OCT and PA imaging.

The use of deformable polymer to confine seeded growth is a new and evolving topic. There are numerous opportunities for further research, including clarification of involved mechanisms, development of more sophisticated control over morphology and composition, and exploration of novel applications of the resulting nanostructures. Future work includes a deeper understanding of how the synthesis and etching conditions determine the cross-linked network and permeability of the confining polymer and how they affect the growth kinetics of the seeds. In addition to TEM and absorbance spectroscopy, more advanced characterization techniques such as liquid cell electron microscopy and real-time small-angle X-ray scattering (SAXS) may be utilized to understand the detailed growth process of the seeds when confined within the polymer nanoshells.

It is important to keep in mind that although RF is a good option for confining the seeded growth, it is not the only choice. The phenolic resin family provides a diverse range of possibilities for further exploration. For instance, different phenolic resins can be created by using various phenol derivatives.[46] By introducing less polar phenol derivatives, such as nonylphenol and dodecyl phenol, the hydrophobic domain percolation inside the resins can be enhanced, compared to resorcinol. These phenolic resins can then be utilized to grow plasmonic nanostructures in oil phases, an area that has not been possible.

Although our previous research has mainly focused on plasmonic nanostructures of noble metals, the principle of the polymer-confined seeded growth process may also be applied to non-noble metals and other compounds. Extending the process to the synthesis of non-noble metals can be readily envisioned, especially for the growth of nanostructures of transition metals such as Fe, Ni, and Co, which feature size- and shape-dependent magnetic properties. However, producing plasmonic nanostructures of non-noble metals such as Al and Mg through this process might pose challenges since their cations are difficult to reduce in solution phases. On the other hand, the current process may be used to grow nanostructures of inorganic compounds, such as perovskite, an emerging semiconductor with great potential for developing high-performance optoelectronic and energy-conversion devices.[62] Previous studies have shown that colloidal perovskite nanostructures can be grown from small seeds. With polymer confinement, it may be possible to grow perovskite seeds into anisotropic shapes typically produced with relatively low morphological controllability through vapor-phase growth on hard templates. Successful implementation of polymer shells not only allows for improvement in morphological control and synthesis robustness but also provides an additional protective layer that enhances the chemical stability of perovskite nanostructures.

AUTHOR INFORMATION

Corresponding Author

Yadong Yin − *Department of Chemistry, University of California, Riverside, California 92521, United States;* orcid.org/0000-0003-0218-3042; Email: yadong.yin@ucr.edu

Authors

Sangmo Liu − *Department of Chemistry, University of California, Riverside, California 92521, United States*

Zuyang Ye − *Department of Chemistry, University of California, Riverside, California 92521, United States*

Complete contact information is available at: https://pubs.acs.org/10.1021/acs.langmuir.4c00706

Notes

The authors declare no competing financial interest.

Biographies

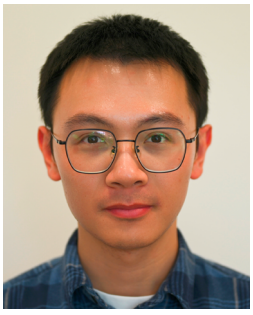

Sangmo Liu is a Ph.D. student at the University of California, Riverside, under the supervision of Prof. Yadong Yin. He received his B.E. in Nanoengineering from Soochow University, China in 2019, and then obtained his M.S. in Bioengineering from the University of Washington, Seattle in 2021. His research work focuses on manipulating heat generation and transfer using magnetic nanostructures.

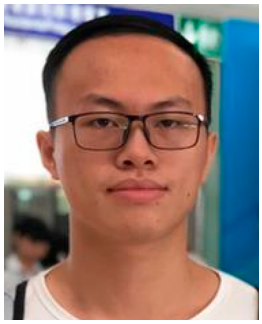

Zuyang Ye is currently a Ph.D. student at the University of California, Riverside, under the supervision of Prof. Yadong Yin. He obtained his B.S. degree in Chemical Physics from the University of Science and Technology of China in 2018. His area of research focuses on the synthesis and assembly of nanostructured materials and their corresponding responsive properties.

https://doi.org/10.1021/acs.langmuir.4c00706
Langmuir 2024, 40, 8760−8770

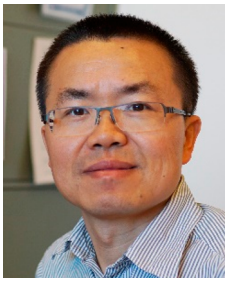

Yadong Yin is a Professor of Chemistry at the University of California, Riverside, with an affiliate appointment in Materials Science and Engineering and Chemical and Environmental Engineering. He received his B.S. and M.S. in Chemistry from the University of Science and Technology of China in 1996 and 1998, respectively, and then a Ph.D. in Materials Science and Engineering from the University of Washington in 2002. In 2003, he worked as a postdoctoral fellow at the University of California, Berkeley, and the Lawrence Berkeley National Laboratory, and then became a staff scientist at the LBNL in 2005. He joined the faculty at the University of California, Riverside, in 2006. He is a recipient of several awards, including the Cottrell Scholar Award (2009), DuPont Young Professor Grant (2010), 3M Nontenured Faculty Grant (2010), NSF CAREER award (2010), NML Researcher Award (2016), MRS Fellow (2020), and the ACS Langmuir Lectureship (2022). His research interests include synthesis, self-assembly, colloidal and interfacial properties, and applications of nanostructured materials.

■ ACKNOWLEDGMENTS

The authors are grateful for the financial support from the U.S. National Science Foundation under Grant No. EEC 1941543.

■ REFERENCES

(1) Ebbesen, T. W.; Lezec, H. J.; Ghaemi, H. F.; Thio, T.; Wolff, P. A. Extraordinary optical transmission through sub-wavelength hole arrays. *Nature* **1998**, *391* (6668), 667−669.
(2) Zeng, S.; Baillargeat, D.; Ho, H.-P.; Yong, K.-T. Nanomaterials enhanced surface plasmon resonance for biological and chemical sensing applications. *Chem. Soc. Rev.* **2014**, *43* (10), 3426−3452.
(3) Li, Z.; Yin, Y. Stimuli-Responsive Optical Nanomaterials. *Adv. Mater.* **2019**, *31* (15), No. 1807061.
(4) Hsu, C. W.; Zhen, B.; Qiu, W.; Shapira, O.; DeLacy, B. G.; Joannopoulos, J. D.; Soljačić, M. Transparent displays enabled by resonant nanoparticle scattering. *Nat. Commun.* **2014**, *5* (1), 3152.
(5) V. Besteiro, L.; Kong, X.-T.; Wang, Z.; Rosei, F.; Govorov, A. O. Plasmonic Glasses and Films Based on Alternative Inexpensive Materials for Blocking Infrared Radiation. *Nano Lett.* **2018**, *18* (5), 3147−3156.
(6) Peng, J.; Jeong, H.-H.; Lin, Q.; Cormier, S.; Liang, H.-L.; De Volder, M. F. L.; Vignolini, S.; Baumberg, J. J. Scalable electrochromic nanopixels using plasmonics. *Science Advances* **2019**, *5* (5), No. eaaw2205.
(7) Lal, S.; Link, S.; Halas, N. J. Nano-optics from sensing to waveguiding. *Nat. Photonics* **2007**, *1* (11), 641−648.
(8) Byers, C. P.; Zhang, H.; Swearer, D. F.; Yorulmaz, M.; Hoener, B. S.; Huang, D.; Hoggard, A.; Chang, W.-S.; Mulvaney, P.; Ringe, E.; Halas, N. J.; Nordlander, P.; Link, S.; Landes, C. F. From tunable core-shell nanoparticles to plasmonic drawbridges: Active control of nanoparticle optical properties. *Science Advances* **2015**, *1* (11), No. e1500988.
(9) Montelongo, Y.; Tenorio-Pearl, J. O.; Williams, C.; Zhang, S.; Milne, W. I.; Wilkinson, T. D. Plasmonic nanoparticle scattering for color holograms. *Proc. Natl. Acad. Sci. U. S. A.* **2014**, *111* (35), 12679−12683.
(10) Chen, T.; Reinhard, B. M. Assembling Color on the Nanoscale: Multichromatic Switchable Pixels from Plasmonic Atoms and Molecules. *Adv. Mater.* **2016**, *28* (18), 3522−3527.
(11) Chen, J.; Feng, J.; Li, Z.; Xu, P.; Wang, X.; Yin, W.; Wang, M.; Ge, X.; Yin, Y. Space-Confined Seeded Growth of Black Silver Nanostructures for Solar Steam Generation. *Nano Lett.* **2019**, *19* (1), 400−407.
(12) Zhou, L.; Tan, Y.; Wang, J.; Xu, W.; Yuan, Y.; Cai, W.; Zhu, S.; Zhu, J. 3D self-assembly of aluminium nanoparticles for plasmon-enhanced solar desalination. *Nat. Photonics* **2016**, *10* (6), 393−398.
(13) Clavero, C. Plasmon-induced hot-electron generation at nanoparticle/metal-oxide interfaces for photovoltaic and photocatalytic devices. *Nat. Photonics* **2014**, *8* (2), 95−103.
(14) Kumar, A.; Kumar, S.; Rhim, W.-K.; Kim, G.-H.; Nam, J.-M. Oxidative Nanopeeling Chemistry-Based Synthesis and Photodynamic and Photothermal Therapeutic Applications of Plasmonic Core-Petal Nanostructures. *J. Am. Chem. Soc.* **2014**, *136* (46), 16317−16325.
(15) Chen, J.; Feng, J.; Yang, F.; Aleisa, R.; Zhang, Q.; Yin, Y. Space-Confined Seeded Growth of Cu Nanorods with Strong Surface Plasmon Resonance for Photothermal Actuation. *Angew. Chem., Int. Ed.* **2019**, *58* (27), 9275−9281.
(16) Huang, P.; Lin, J.; Li, W. W.; Rong, P. F.; Wang, Z.; Wang, S. J.; Wang, X. P.; Sun, X. L.; Aronova, M.; Niu, G.; Leapman, R. D.; Nie, Z. H.; Chen, X. Y. Biodegradable Gold Nanovesicles with an Ultrastrong Plasmonic Coupling Effect for Photoacoustic Imaging and Photothermal Therapy. *Angew. Chem. Int. Edit* **2013**, *52* (52), 13958−13964.
(17) Li, Z.; Yin, S.; Cheng, L.; Yang, K.; Li, Y.; Liu, Z. Magnetic Targeting Enhanced Theranostic Strategy Based on Multimodal Imaging for Selective Ablation of Cancer. *Adv. Funct. Mater.* **2014**, *24* (16), 2312−2321.
(18) Jiang, N.; Zhuo, X.; Wang, J. Active Plasmonics: Principles, Structures, and Applications. *Chem. Rev.* **2018**, *118* (6), 3054−3099.
(19) Millstone, J. E.; Park, S.; Shuford, K. L.; Qin, L.; Schatz, G. C.; Mirkin, C. A. Observation of a Quadrupole Plasmon Mode for a Colloidal Solution of Gold Nanoprisms. *J. Am. Chem. Soc.* **2005**, *127* (15), 5312−5313.
(20) Eustis, S.; El-Sayed, M. A. Determination of the aspect ratio statistical distribution of gold nanorods in solution from a theoretical fit of the observed inhomogeneously broadened longitudinal plasmon resonance absorption spectrum. *J. Appl. Phys.* **2006**, *100* (4), No. 044324.
(21) Zhang, Q.; Ge, J.; Pham, T.; Goebl, J.; Hu, Y.; Lu, Z.; Yin, Y. Reconstruction of Silver Nanoplates by UV Irradiation: Tailored Optical Properties and Enhanced Stability. *Angew. Chem., Int. Ed.* **2009**, *48* (19), 3516−3519.
(22) Goebl, J.; Zhang, Q.; He, L.; Yin, Y. Monitoring the Shape Evolution of Silver Nanoplates: A Marker Study. *Angew. Chem., Int. Ed.* **2012**, *51* (2), 552−555.
(23) Gao, C. B.; Zhang, Q.; Lu, Z. D.; Yin, Y. D. Templated Synthesis of Metal Nanorods in Silica Nanotubes. *J. Am. Chem. Soc.* **2011**, *133* (49), 19706−19709.
(24) Gao, C.; Goebl, J.; Yin, Y. Seeded growth route to noble metal nanostructures. *Journal of Materials Chemistry C* **2013**, *1* (25), 3898−3909.
(25) Liu, Q.; Cui, Y.; Gardner, D.; Li, X.; He, S.; Smalyukh, I. I. Self-Alignment of Plasmonic Gold Nanorods in Reconfigurable Anisotropic Fluids for Tunable Bulk Metamaterial Applications. *Nano Lett.* **2010**, *10* (4), 1347−1353.
(26) Liu, Q.; Yuan, Y.; Smalyukh, I. I. Electrically and Optically Tunable Plasmonic Guest−Host Liquid Crystals with Long-Range Ordered Nanoparticles. *Nano Lett.* **2014**, *14* (7), 4071−4077.
(27) Li, Z.; Jin, J.; Yang, F.; Song, N.; Yin, Y. Coupling magnetic and plasmonic anisotropy in hybrid nanorods for mechanochromic responses. *Nat. Commun.* **2020**, *11* (1), 2883.
(28) Li, Z.; Poon, W.; Ye, Z.; Qi, F.; Park, B. H.; Yin, Y. Magnetic Field-Modulated Plasmonic Scattering of Hybrid Nanorods for FFT-

https://doi.org/10.1021/acs.langmuir.4c00706
Langmuir 2024, 40, 8760−8770

Weighted OCT Imaging in NIR-II. *ACS Nano* **2022**, *16* (8), 12738−12746.
(29) Li, Z.; Meng, Z.; Tian, F.; Ye, Z.; Zhou, X.; Zhong, X.; Chen, Q.; Yang, M.; Liu, Z.; Yin, Y. Fast Fourier Transform-weighted Photoacoustic Imaging by In Vivo Magnetic Alignment of Hybrid Nanorods. *Nano Lett.* **2022**, *22* (13), 5158−5166.
(30) Maity, S.; Wu, W.-C.; Tracy, J. B.; Clarke, L. I.; Bochinski, J. R. Nanoscale steady-state temperature gradients within polymer nanocomposites undergoing continuous-wave photothermal heating from gold nanorods. *Nanoscale* **2017**, *9* (32), 11605−11618.
(31) Li, Z. W.; Ye, Z. Y.; Han, L. L.; Fan, Q. S.; Wu, C. L.; Ding, D.; Xin, H. L. L.; Myung, N. V.; Yin, Y. D. Polarization-Modulated Multidirectional Photothermal Actuators. *Adv. Mater.* **2021**, *33* (3), No. 2006367.
(32) Jana, N. R.; Gearheart, L.; Murphy, C. J. Seed-Mediated Growth Approach for Shape-Controlled Synthesis of Spheroidal and Rod-like Gold Nanoparticles Using a Surfactant Template. *Adv. Mater.* **2001**, *13* (18), 1389−1393.
(33) Nikoobakht, B.; El-Sayed, M. A. Preparation and Growth Mechanism of Gold Nanorods (NRs) Using Seed-Mediated Growth Method. *Chem. Mater.* **2003**, *15* (10), 1957−1962.
(34) Bastús, N. G.; Merkoçi, F.; Piella, J.; Puntes, V. Synthesis of Highly Monodisperse Citrate-Stabilized Silver Nanoparticles of up to 200 nm: Kinetic Control and Catalytic Properties. *Chem. Mater.* **2014**, *26* (9), 2836−2846.
(35) Sun, Y.; Xia, Y. Large-Scale Synthesis of Uniform Silver Nanowires Through a Soft, Self-Seeding, Polyol Process. *Adv. Mater.* **2002**, *14* (11), 833−837.
(36) Habas, S. E.; Lee, H.; Radmilovic, V.; Somorjai, G. A.; Yang, P. Shaping binary metal nanocrystals through epitaxial seeded growth. *Nat. Mater.* **2007**, *6* (9), 692−697.
(37) Xia, Y.; Xiong, Y.; Lim, B.; Skrabalak, S. E. Shape-Controlled Synthesis of Metal Nanocrystals: Simple Chemistry Meets Complex Physics? *Angew. Chem., Int. Ed.* **2009**, *48* (1), 60−103.
(38) Zhang, Q.; Li, N.; Goebl, J.; Lu, Z.; Yin, Y. A Systematic Study of the Synthesis of Silver Nanoplates: Is Citrate a "Magic" Reagent? *J. Am. Chem. Soc.* **2011**, *133* (46), 18931−18939.
(39) Chen, L.; Ji, F.; Xu, Y.; He, L.; Mi, Y.; Bao, F.; Sun, B.; Zhang, X.; Zhang, Q. High-Yield Seedless Synthesis of Triangular Gold Nanoplates through Oxidative Etching. *Nano Lett.* **2014**, *14* (12), 7201−7206.
(40) Liu, X.; Yin, Y.; Gao, C. Size-Tailored Synthesis of Silver Quasi-Nanospheres by Kinetically Controlled Seeded Growth. *Langmuir* **2013**, *29* (33), 10559−10565.
(41) Jin, M.; Zhang, H.; Wang, J.; Zhong, X.; Lu, N.; Li, Z.; Xie, Z.; Kim, M. J.; Xia, Y. Copper Can Still Be Epitaxially Deposited on Palladium Nanocrystals To Generate Core−Shell Nanocubes Despite Their Large Lattice Mismatch. *ACS Nano* **2012**, *6* (3), 2566−2573.
(42) Liu, Y.; Goebl, J.; Yin, Y. Templated synthesis of nanostructured materials. *Chem. Soc. Rev.* **2013**, *42* (7), 2610−2653.
(43) Li, Z.; Zhang, J.; Jin, J.; Yang, F.; Aleisa, R.; Yin, Y. Creation and Reconstruction of Thermochromic Au Nanorods with Surface Concavity. *J. Am. Chem. Soc.* **2021**, *143* (38), 15791−15799.
(44) Chen, J.; Bai, Y.; Feng, J.; Yang, F.; Xu, P.; Wang, Z.; Zhang, Q.; Yin, Y. Anisotropic Seeded Growth of Ag Nanoplates Confined in Shape-Deformable Spaces. *Angew. Chem., Int. Ed.* **2021**, *60* (8), 4117−4124.
(45) Li, T.; Cao, M.; Liang, J.; Xie, X.; Du, G. Mechanism of Base-Catalyzed Resorcinol-Formaldehyde and Phenol-Resorcinol-Formaldehyde Condensation Reactions: A Theoretical Study. *Polymers (Basel)* **2017**, *9* (9), 426.
(46) Shiraishi, Y.; Takii, T.; Hagi, T.; Mori, S.; Kofuji, Y.; Kitagawa, Y.; Tanaka, S.; Ichikawa, S.; Hirai, T. Resorcinol−formaldehyde resins as metal-free semiconductor photocatalysts for solar-to-hydrogen peroxide energy conversion. *Nat. Mater.* **2019**, *18* (9), 985−993.
(47) Huang, J. P.; Kwei, T. K.; Reiser, A. The dissolution of novolak in aqueous alkali. *Macromolecules* **1989**, *22* (10), 4106−4112.
(48) Yeh, T. F.; Shih, H. Y.; Reiser, A. Percolation view of novolak dissolution and dissolution inhibition. *Macromolecules* **1992**, *25* (20), 5345−5352.
(49) Gao, Z.; Eisenberg, A. A model of micellization for block copolymers in solutions. *Macromolecules* **1993**, *26* (26), 7353−7360.
(50) Shih, H.-Y.; Reiser, A. A Percolation View of Novolak Dissolution. 4. Mechanism of Inhibitor Action. *Macromolecules* **1995**, *28* (16), 5595−5600.
(51) Pierre, A. C.; Pajonk, G. M. Chemistry of Aerogels and Their Applications. *Chem. Rev.* **2002**, *102* (11), 4243−4266.
(52) Liu, J.; Qiao, S. Z.; Liu, H.; Chen, J.; Orpe, A.; Zhao, D.; Lu, G. Q. Extension of The Stöber Method to the Preparation of Monodisperse Resorcinol−Formaldehyde Resin Polymer and Carbon Spheres. *Angew. Chem., Int. Ed.* **2011**, *50* (26), 5947−5951.
(53) Zhou, S.; Bai, Y.; Xu, W.; Feng, J.; Wang, X.; Li, Z.; Yin, Y. Formation of resorcinol-formaldehyde hollow nanoshells through a dissolution−regrowth process. *Nanoscale* **2020**, *12* (28), 15460−15465.
(54) Li, N.; Zhang, Q.; Liu, J.; Joo, J.; Lee, A.; Gan, Y.; Yin, Y. Sol−gel coating of inorganic nanostructures with resorcinol−formaldehyde resin. *Chem. Commun.* **2013**, *49* (45), 5135−5137.
(55) Izumi, A.; Nakao, T.; Shibayama, M. Atomistic molecular dynamics study of cross-linked phenolic resins. *Soft Matter* **2012**, *8* (19), 5283−5292.
(56) Zhang, J.; Li, Z.; Bai, Y.; Yin, Y. Gold nanocups with multimodal plasmon resonance for quantum-dot random lasing. *Applied Materials Today* **2022**, *26*, No. 101358.
(57) Xianyu, Y.; Lin, Y.; Chen, Q.; Belessiotis-Richards, A.; Stevens, M. M.; Thomas, M. R. Iodide-Mediated Rapid and Sensitive Surface Etching of Gold Nanostars for Biosensing. *Angew. Chem., Int. Ed.* **2021**, *60* (18), 9891−9896.
(58) Chen, J.; Gong, M.; Fan, Y.; Feng, J.; Han, L.; Xin, H. L.; Cao, M.; Zhang, Q.; Zhang, D.; Lei, D.; Yin, Y. Collective Plasmon Coupling in Gold Nanoparticle Clusters for Highly Efficient Photothermal Therapy. *ACS Nano* **2022**, *16* (1), 910−920.
(59) Radloff, C.; Halas, N. J. Plasmonic Properties of Concentric Nanoshells. *Nano Lett.* **2004**, *4* (7), 1323−1327.
(60) Li, Z.; Myung, N. V.; Yin, Y. Light-powered soft steam engines for self-adaptive oscillation and biomimetic swimming. *Science Robotics* **2021**, *6* (61), No. eabi4523.
(61) Li, Z.; Fan, Q.; Wu, C.; Li, Y.; Cheng, C.; Yin, Y. Magnetically Tunable Plasmon Coupling of Au Nanoshells Enabled by Space-Free Confined Growth. *Nano Lett.* **2020**, *20* (11), 8242−8249.
(62) Chen, J.; Zhou, Y.; Fu, Y.; Pan, J.; Mohammed, O. F.; Bakr, O. M. Oriented Halide Perovskite Nanostructures and Thin Films for Optoelectronics. *Chem. Rev.* **2021**, *121* (20), 12112−12180.

https://doi.org/10.1021/acs.langmuir.4c00706
Langmuir 2024, 40, 8760−8770